

# CLIC LUMINOSITY MONITORING

Armen Apyan\*, CERN, Geneva, Switzerland and Northwestern University, Evanston, IL, USA  
 Lawrence Charles Deacon, Edda Gschwendtner, Thibaut Lefevre, CERN, Geneva, Switzerland  
 Robert B. Appleby, Sam Tygier†, The University of Manchester and the Cockcroft Institute, UK

## Abstract

The CLIC post-collision line is designed to transport the un-collided beams and the products of the collided beams with a total power of 14 MW to the main beam dump. Luminosity monitoring for CLIC is based on high energy muons produced by beamstrahlung photons in the main dump. Threshold Cherenkov counters are proposed for the detection of these muons. The expected rates and layout for these detectors is presented. Another method for luminosity monitoring is to directly detect the beamstrahlung photons in the post-collision line. Full Monte Carlo simulation has been performed to address its feasibility.

## INTRODUCTION

The 1.5 TeV electron/positron CLIC beams must be focused to nanometer spot sizes in the interaction point (IP) to reach the required luminosity. The resulting strong beam-beam effects lead to a strong emittance growth for the outgoing beams as well as to the production of beamstrahlung photons and  $e^+e^-$  pairs. There is a strong dependence of the beam deflection angle on the offsets between the bunches. The beam receives deflection, opposite to its direction of offset, after colliding with the second beam with opposite charge.

The post-collision lines (PCL) are designed to transport, from the interaction point to the main beam dump, both the un-collided beams as well as the collided beams with their increased momentum spread and angular divergence [1, 2, 3].

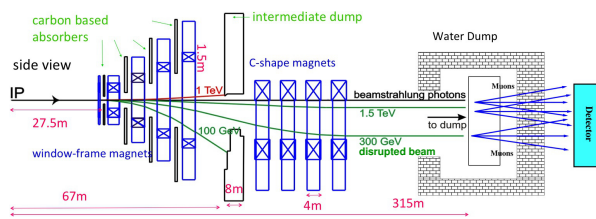


Figure 1: Baseline layout of the post-collision line.

The baseline layout of the CLIC PCL is shown in Fig. 1. The line ends with a main dump at 315 m from the IP, designed to dump the main beam particles, the high energy tail of the beam-beam charged particles (pairs) and the beamstrahlung photons. A significant portion of the pairs are stopped in an intermediate dump, located 67 m from the IP. The post-collision line contains eight dipoles - four located on the IP-side of the intermediate dump, and four

located in the region after the intermediate dump. In order to be able to use the beamstrahlung photons as a luminosity monitoring signal, the conceptual design for the CLIC PCL includes a vertical separation of the beamstrahlung photons from the disrupted electron beam and  $e^+e^-$  coherent pairs of about 12 cm [1] by a magnetic chicane.

Two independent techniques for the luminosity monitoring in the CLIC PCL are proposed and discussed in [4]. Further detailed Monte-Carlo simulations on the detection of the beam-beam collision products are presented in this paper. The types and possible locations of the detectors are also discussed.

## SIMULATION RESULTS OF LUMINOSITY MONITORING SYSTEM

The main beam dump luminosity monitors are positioned behind the main beam dump with the additional shielding to reject possible remaining low energy background. The technique is based on the detection of the high energy muon pairs produced by dumped particles and radiation [4]. The positions of muons produced in the dump are affected by the transverse offsets between the beams at collision.

A double gaussian fit was used to determine the peak position of the muon distribution in the vertical and horizontal directions. The summary for the vertical direction is presented in Fig. 2. The red and blue data points correspond to the muons produced by the disrupted beam and the beamstrahlung photons respectively.

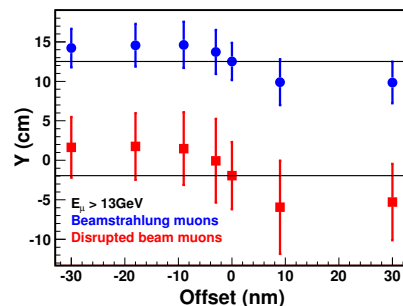


Figure 2: Peak position of muons distribution produced by disrupted beam (red) and beamstrahlung photons (blue) depending on the offsets of colliding beams

## Muon Detector Simulation

We consider a threshold Cherenkov muon detector array consisting of helium gas-filled aluminum tubes with

\* Armen.Apyan@cern.ch

† Sam.Tygier@hep.manchester.ac.uk

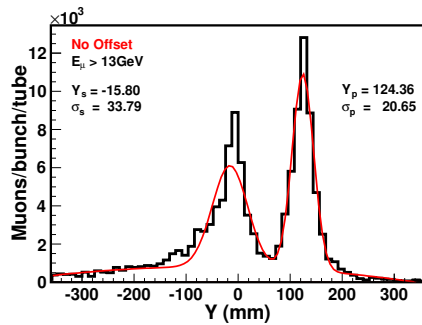


Figure 3: Vertical distribution of the muons entering Cherenkov tubes with  $x = 6$  mm.

0.1 mm thick entrance and exit windows placed downstream of the the main dump rear concrete shielding. The considered detector should be designed to cover  $80\text{ cm} \times 80\text{ cm}$  area to have a full picture of the spatial distribution of the muons. Helium gas has a good transparency and small refractive index ( $n = 1.000036$ ) at standard temperature and pressure (STP). It has a rather high  $\sim 13$  GeV energy threshold at STP for detecting the muon pairs. The Cherenkov light output is 0.2-3.6 photons/m for muons with energy 13-50 GeV with the maximum emission angle of 0.1-0.46 degree. Detection of muons after the main dump by Cherenkov counters was simulated using GEANT4 [5] using the collision product data from [6].

Fig. 3 shows the number of muons entering the set of tubes centered at  $x = 6$  mm.

Fig. 4 shows the number of Cherenkov photons produced in the same set of tubes as in Fig. 3.

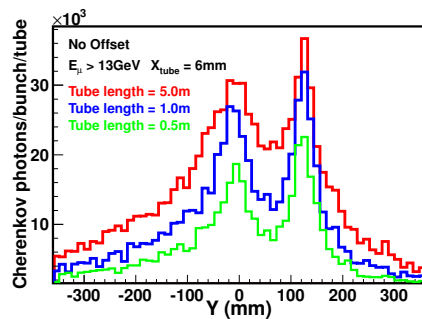


Figure 4: Vertical distribution of Cherenkov photons at the rear window of tubes with  $x = 6$  mm.

Table 1 shows the fit results of distribution of muons entering the tubes and Cherenkov photons (Ch.Ph.) depending on the tube length.

Several different tube diameters ranging from 10 mm to 150 mm were considered. From a preliminary inspection of the simulation results it appears that the resolution is poor for the Cherenkov tubes with larger diameters. Potentially useful information could be extracted from the structure of the spatial distribution using tubes of diameter 10 mm as shown in Fig. 5. The left plot shows the spatial distribution of the muons downstream of main beam dump in case

of head on collision. The central and right plots show the corresponding yield of Cherenkov photons for 1 m and 5 m tubes.

Table 1: Fit Results of Muons and Cherenkov Photons Distribution

	Tube length	Spent Beam	Beamstrahlung Photons
Muon	—	$-15.8 \pm 33.8$ mm	$124.4 \pm 20.7$ mm
Ch. Ph.	0.5 m	$-11.1 \pm 41.7$ mm	$124.4 \pm 24.0$ mm
Ch. Ph.	1.0 m	$-13.1 \pm 42.3$ mm	$124.2 \pm 23.8$ mm
Ch. Ph.	2.0 m	$-14.3 \pm 49.1$ mm	$125.4 \pm 27.5$ mm
Ch. Ph.	5.0 m	$-11.9 \pm 53.8$ mm	$125.1 \pm 28.2$ mm

### Beamstrahlung Photons Detection

There are a number of potential sites for photon detectors in the PCL. The following were considered: directly before or after the intermediate dump, at 66 m or 76 m, after the C magnets at 109 m, and midway along the final straight at 200 m. Monte Carlo simulations were carried out with FLUKA [7] using the collision product data from [6]. The model geometry was updated from previous work [4] to include magnet coils, tunnel walls and soil, and to update the dump geometry. Benchmarking energy deposition against previous studies and a BDSIM/GEANT model is ongoing. The main loss locations are shown in table 2.

Table 2: Beam Loss at Elements, in Watts

	Spent Beam	Photons	Co+	Co -
MainDump	9.94 M	3.60 M	97.76 K	93.50
IntDump	57.47 K	114.10	19.37 K	124.54 K
Mask1	18.42	2.43	3.44	80.95
Mask2	202.60	0.00	140.68	425.84
Mask3	1.12 K	0.00	836.52	632.48
Mask4	3.03 K	0.00	1.67 K	1.53 K

Production cuts were set to equivalent energies of 50 cm range cuts in GEANT4. Photo-nuclear interactions were enabled. Simulations were run for a selection of collision offsets. All particles crossing the above planes were recorded, so that detector geometry could be adjusted without rerunning the simulation.

The total power of the beamstrahlung photons is around 3.6 MW, so any detector must be placed in the tails of the distribution to avoid damage. The detector must also be positioned to avoid the disrupted beam, which is separated downwards by the first set of magnets.

A photon detector before the intermediate dump, for example at 66 m, can be ruled out because the beamstrahlung cone overlaps the opposite sign coherent pairs which have been bent upwards by the first bend. These backgrounds are partially removed by the intermediate dump, favouring a detector at 109 m (beyond the intermediate dump).

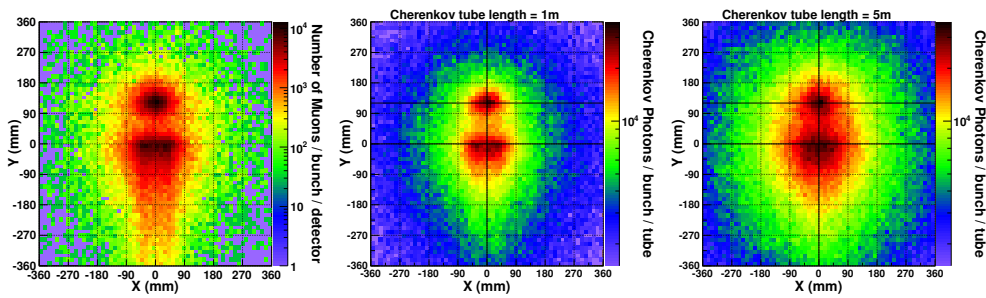


Figure 5: Spatial distribution of muons on the face of Cherenkov array monitor (left figure) and Cherenkov photons at exit window of the tubes (right two figures).

For example, a  $10 \times 10$  cm detector, centred 10 cm above the photon cone centre at 109 m would receive  $1.5 \times 10^7$  photons above 1 MeV per bunch crossing, with an mean energy of 9.6 GeV.

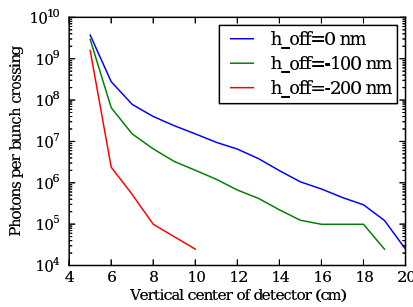


Figure 6: The photon count at a 10 cm photon counter located at 109 m from the IP as a function of the vertical offset of the counter, for three different horizontal IP beam-beam offsets.

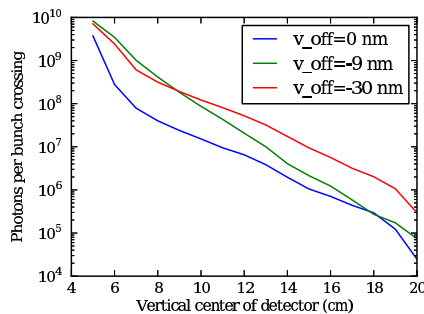


Figure 7: The photon count at a 10 cm photon counter located at 109 m from the IP as a function of the vertical offset of the counter, for three different vertical IP beam-beam offsets.

Fig. 6 shows how the photon count in a 10 cm photon counter located at 109 m from the IP changes as a function of the vertical offset of the counter from the photon cone, for several beam-beam horizontal collision offsets. Fig. 7 shows the same for vertical collision offsets. The

correlation of the photon count at this location with horizontal IP beam-beam offsets (linked to effective luminosity) is clearly seen. The influence of background on photon detectors at this location is under study.

### CONCLUSION

The simulation results for the luminosity monitoring in the CLIC PCL are presented. The simulations suggest that the gaseous threshold Cherenkov arrays are capable to detect the change in the collision product distribution caused by the offsets of colliding bunches.

Direct measurement of the beamstrahlung photons in the PCL has also been studied. There are several candidate locations for photon detectors after the intermediate dump, where the background from direct coherent pairs is reduced. These have offset dependent signals. Detailed studies of backgrounds and Cherenkov muon array are ongoing.

### ACKNOWLEDGMENT

The research leading to these results has received funding from the European Commission under the FP7 Research Infrastructures project EuCARD, grant agreement no.227579.

### REFERENCES

- [1] E. Gschwendtner *et al.*, in Proc. of IPAC10 Conference, Kyoto, 2010, WEPE019, 3386 (2010).
- [2] M.D. Salt *et al.*, in Proc. of IPAC10 Conference, Kyoto, 2010, WEPE020, 3389 (2010).
- [3] A. Ferrari *et al.*, Phys. Rev. ST Accel. Beams **62**, 021001 (2009).
- [4] R. B. Appleby *et al.*, in Proc. of IPAC2011, San Sebastian, Spain, TUPC027 (2011).
- [5] S. Agostinelli *et al.*, GEANT4 - a simulation toolkit, Nucl. Instr. and Meth. Phys. A **506**, 250 (2003).
- [6] B. Dalena, private communication.
- [7] G. Battistoni *et al.*, The FLUKA code: Description and benchmarking, in Proc. of the Hadronic Shower Simulation Workshop 2006, Fermilab 2006, M. Albrow, R. Raja eds., AIP Conference Proceeding 896, 31 (2007).